

Temperature Measurements of Microhotplates Using Fluorescence Thermometry

C.W. Meyer, D.C. Meier, C. B. Montgomery, and S. Semancik

*Chemical Science and Technology Laboratory
National Institute of Standards and Technology
Gaithersburg, MD*

Abstract: A fluorescence microscope has been constructed for measuring surface temperatures of microhotplate platforms. The microscope measures temperature-dependent fluorescence lifetimes of a film of the phosphor $\text{Mg}_4(\text{F})\text{GeO}_6:\text{Mn}$ which is deposited on the microhotplate. Temperature/fluorescence-lifetime relations for this phosphor are determined by measuring the fluorescence lifetime of the phosphor-coated hot junction of a type S thermocouple while controlling and monitoring its temperature. These fluorescence-lifetime measurements have been used to determine the average temperature of microhotplates. Studies have been performed on the temperature stability of the microhotplates under steady heating and on the reproducibility of the temperatures achieved under thermal cycling. Fluorescence-intensity thermometry has been used to measure the thermal response time of microhotplates. This work demonstrates the potential of fluorescence thermometry for characterizing microhotplate performance.

I. Introduction

MEMS devices called “microhotplates”, which are fabricated by micromachining silicon, have emerged in recent years as an important tool for temperature-controlled conductometric gas sensing [1]. These microsensors, typically $100\ \mu\text{m} \times 100\ \mu\text{m}$, feature a resistive heater (metal thin-film or embedded polysilicon) deposited on them and are coated with a semiconducting chemical-sensing film. A diagram and SEM micrograph of a typical microhotplate are shown in Figure 1. The electrical conductance of these microhotplate sensing films is a function of the gas adsorption/desorption and reaction-behavior at the surface of the sensing film, which depends on temperature. When the temperature of these microhotplates is modulated, the conductance response can provide time-dependent information on the surface adsorbates. Because of the large role that proper temperature control and measurement play in this process, they are important to the success of microhotplates as chemical sensors.

Microhotplate temperatures are generally determined by measuring the electrical resistance of the heater [1]. The temperature/resistance relations are obtained by measuring the resistance while the microhotplate is situated in a stable environment with a known temperature. Unfortunately temperature measurement using heater resistance provides no information on the temperature distribution across the surface of the microhotplate. Also, temperature gradients between the heater and sensing film may result in the heater temperature being somewhat unrepresentative of the actual sensing-film temperature during rapid thermal cycling. Therefore, it is important to find other methods for measuring the surface temperature of microhotplates. Measurements are also needed to provide the specific temperatures where features are observed in temperature-programmed sensing operation signatures [1,2] and better define critical thermal

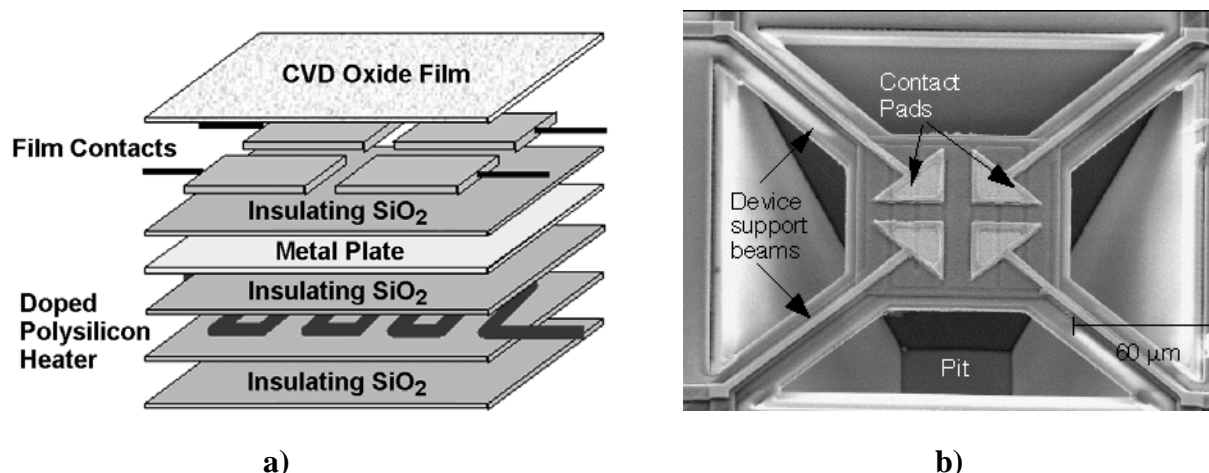


Figure 1. a) Cross section of layer structure of a typical microhotplate. b) SEM micrograph of microhotplate before deposition of oxide film.

regimes when microhotplate arrays are used in materials processing and performance studies [3,4].

Fluorescence thermometry has been studied for decades as a tool for noncontact surface temperature measurement [5]. In this technique, the surface for which the temperature is to be measured is coated with a thin layer of a phosphor whose fluorescence intensity and fluorescence lifetime are temperature dependent. Fluorescence is excited by illuminating a small area of the phosphor. A fluorescence-intensity thermometer uses steady illumination and measures the fluorescence intensity with a photomultiplier (PMT) tube [5] to determine the temperature of the phosphor. A fluorescence-lifetime thermometer provides time-dependent illumination to the area and analyzes the measured time-dependent fluorescence intensity to determine the fluorescence lifetime [5]. While fluorescence-intensity thermometry is easier to perform, fluorescence-lifetime thermometry is generally more reliable because the measured quantity (lifetime) does not need to be normalized.

Recently these fluorescence thermometry techniques have been implemented using microscopes to achieve temperature measurement of very small surface areas [6-10], and these methods can be used to make surface-temperature measurements on microhotplate platforms. Fluorescence thermometry can be used for both static and dynamic temperature measurements. While chemical sensing cannot be performed with the phosphor film coating the microhotplate, fluorescence thermometry can be useful for validating (or determining) the temperature/heater-resistance relations of the microhotplate and for improving microhotplate heater designs to make microhotplate surface temperatures more uniform. It can also be used to measure the dynamic response of the surface temperature to time-dependent heating.

In this paper we present results of surface-temperature measurements on a microhotplate using fluorescence thermometry with the phosphor Mg₄(F)GeO₆:Mn. The fluorescence microscope and the method for measuring the fluorescence lifetime are described. The technique for determining the phosphor's temperature/fluorescence-lifetime relations using a type S thermo-

couple is discussed, as well as the uncertainty of temperature measurements in this system. Afterwards, we show measurements of the stability of microhotplate surface temperatures under steady heating. We also show measurements of the reproducibility of temperatures achieved under pulsed heating. Finally we use fluorescence intensity thermometry to determine the response time of microhotplate surface temperatures to pulsed heating.

II. Fluorescence Microscope

The fluorescence-lifetime microscope was constructed by mounting a blue LED ($\lambda_{\text{peak}} = 470 \text{ nm}$) [8,11] in the microscope to provide excitation illumination to the phosphor. A wave generator provided power to the LED. An interference filter with a 60 nm bandwidth and a transmission peak centered at $\lambda = 450 \text{ nm}$ was placed in front of the LED to minimize excitation illumination at the fluorescence wavelength. The LED radiation was directed horizontally onto a beamsplitter in the microscope, which directed the radiation downwards. A plano-convex lens with focal length 12 mm was placed between the interference filter and beamsplitter and focused the radiation on the area within the field of view of the microscope. The resulting fluorescence radiation was directed upwards through the beamsplitter to a PMT that was mounted on top of the microscope. This PMT measured the intensity of the fluorescence, which had a peak wavelength of $\lambda_{\text{peak}} = 658 \text{ nm}$. An interference filter with a 10 nm bandwidth and a transmission peak centered at $\lambda = 656 \text{ nm}$ was placed below the PMT to prevent stray (non-fluorescent) radiation from reaching it. A current amplifier was used to improve the signal from the PMT.

The fluorescence lifetime was measured using frequency-domain fluorometry [12]. To measure the fluorescence lifetime, the voltage applied to the LED was modulated using a sine function with frequency $\omega/2\pi = 50 \text{ Hz}$, and a signal analyzer (Agilent 35660A [13]) measured the phase shift at ω of the fluorescence radiation from that of the voltage applied to the LED. The lifetime τ was then calculated using the equation

$$\tau = \tan(\phi - \phi_0) / \omega \quad 1)$$

where ϕ is the phase shift between the measured fluorescence radiation and the voltage applied to the LED and ϕ_0 is the measured phase shift between the measured LED radiation and the voltage applied to the LED. The value of ϕ_0 had been measured at an earlier time by placing a non-fluorescent material under the microscope and removing the interference filter below the PMT; for a given LED modulation amplitude and frequency, ϕ_0 was assumed to remain constant. The difference $\phi - \phi_0$ is the phase shift between the fluorescent radiation and the LED radiation.

III. Phosphor Temperature/Fluorescence-Lifetime Relations

The phosphor used was $\text{Mg}_4(\text{F})\text{GeO}_6:\text{Mn}$, which fluoresces at $\lambda_{\text{peak}} = 658 \text{ nm}$ and has been frequently used for fluorescence thermometry over the range $0 \text{ }^\circ\text{C}$ to $450 \text{ }^\circ\text{C}$ [5]. For calibration and characterization studies, the phosphor was coated on the hot junction of a type S thermocouple using a chemical binder. Before coating, the junction was mashed to produce a flat surface.

The calibrating thermocouple was mounted in a cylindrical two-bore alumina insulator that was 10 cm long and had 3 mm outer diameter. The thermocouple wires were 0.5 mm in diameter and were located inside the bores. The wires were annealed before the thermocouple was assembled. The thermocouple was uncalibrated, so the reference function for type S thermocouples was used [14]. The expanded uncertainty ($k=2$) of temperature measurement using such a technique is 1.7 °C [14], but the reproducibility is better than 0.1 °C.

The temperature of the thermocouple's hot junction was controlled by inserting it into a horizontal well in a temperature-controlled copper disk. The diameter of the disk was 7.6 cm and its thickness was 1.8 cm. The well was 3.2 mm in diameter and was 7 cm deep. The axis of the well was 2 mm below the top of the disk. A 2 mm diameter hole was drilled from the top of the disk to the well at a depth of 3.8 cm into the well so that the embedded thermocouple's hot junction could be visually observed from above. The disk had a wire heater wrapped around it and was surrounded by 1.2 cm of insulation on the bottom and sides. The disk and insulation were enclosed in a hollow, topless cylindrical brass container in thermal contact with water-cooled tubes around its periphery. A PID controller was used to control the disk's temperature to ± 0.1 °C at temperatures from 23 °C to 450 °C. For its sensor, the controller used a second type S thermocouple, identical to the calibration thermocouple described above and located in an adjacent well. The brass container could be mounted under the fluorescence microscope to enable simultaneous measurements of the temperature and fluorescence lifetime.

The fluorescence-lifetime/temperature relations were measured for $\text{Mg}_4(\text{F})\text{GeO}_6:\text{Mn}$ over the range 23 °C to 450 °C. This was achieved by mounting the temperature-controlled disk under the fluorescence microscope such that the hole from the top of the disk to the calibration thermocouple well was within the field of view of the microscope. The thermocouple was placed in the well so that the phosphor-coated hot junction of the thermocouple was underneath the hole and within the field of view. The thermocouple was oriented so that the mashed hot junction was horizontal, providing a flat disk of ~ 1 mm diameter on which the microscope could focus. The microscope magnification was 16 \times and the hot junction filled the entire field of view. The thermocouple was referenced to an ice bath and its emf was measured with an 8-digit multimeter to determine the temperature of the hot junction. For each temperature, the thermocouple hot-junction temperature and the phosphor lifetime were simultaneously measured every 10 s for a period of 300 s. The temperature and lifetime values were then averaged over this period. The results of the measurements are shown in Figure 2. The measurements are shown as solid circles and the curve is a 7th order polynomial fit. The residuals to this fit, shown in Figure 2b, are all within ± 1 °C.

Figure 3 shows a comparison between the temperatures measured by the calibration thermocouple and by fluorescence thermometry using the calibration shown in Fig. 2. The experimental system described above was used with a steady heating of the copper disk at 425 °C. In Fig. 3, an offset of 0.3 °C was added to the fluorescence thermometry measurements for better viewing of how the two temperatures track each other. The agreement is remarkable considering that one technique is through contact thermometry and the other is non-contact. The resolution is 0.05 °C in this plot; in general it was found to be strongly dependent on the experimental configuration, particularly the intensity of the excitation illumination. Short-term repeatability tests on the phosphor lifetime were performed by cycling the thermocouple junction

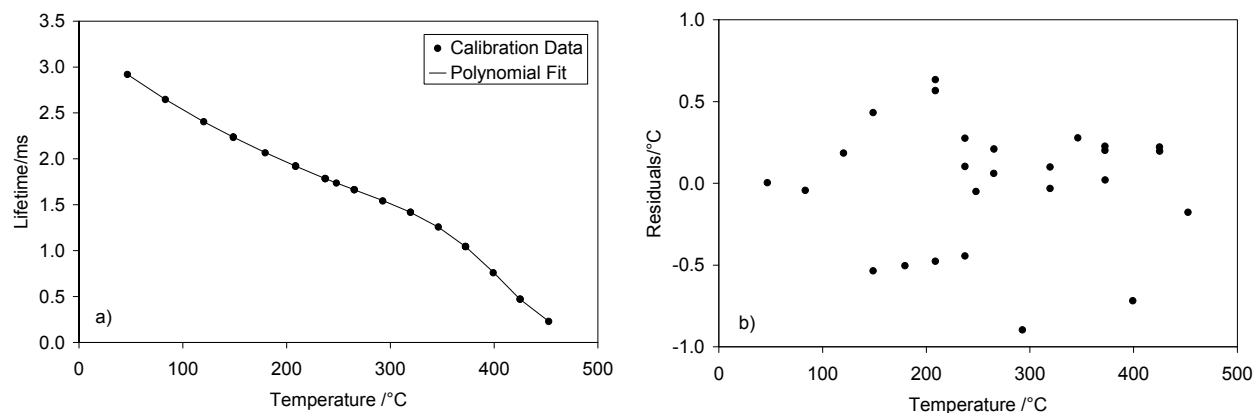


Figure 2. a) Fluorescence-lifetime/temperature relations measured for $\text{Mg}_4(\text{F})\text{GeO}_6:\text{Mn}$. The data is shown as solid circles and the curve is a 7th order polynomial fit. b) Residuals from the polynomial fit shown in a).

temperature from 240 °C to room temperature and back several times; the repeatability was shown to be within 0.2 °C.

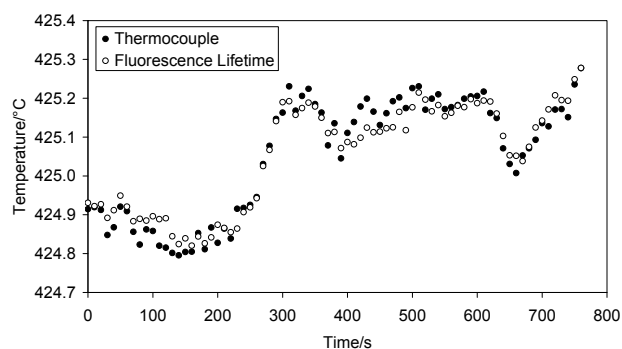


Figure 3. Comparison of temperatures measured by the thermocouple (solid circles) and fluorescence-lifetime thermometry (open circles). An offset of 0.3 °C was added to the fluorescence data.

The resolution of the temperature measurements was found to be dependent upon the signal-to-noise ratio from the PMT. This is determined by the intensity of fluorescence, which is increased with higher excitation illumination provided to the phosphor. While the best resolution obtained was 0.05 °C, more intense illumination should increase this resolution even more. The uncertainty of the temperature measurements from this system was studied by reproducibility tests. In these tests, the phosphor film was scraped off of the thermocouple junction after a calibration was performed and a second film was then applied. Afterwards a second calibration was performed, and the two were compared. An example is shown in Fig. 4. In Fig. 4a, the fluorescence lifetime as a function of temperature is shown for two different phosphor films, where the solid circles are the results shown in Fig. 2. In Fig. 4b, the difference between the two calibration results, displayed as a temperature difference, is shown as a function of temperature. The temperature difference is largest (32 °C) at the lowest temperature and decreases as the temperature is increased; above 300 °C the difference is within 1.5 °C.

The lifetime differences observed in Fig. 4a are probably due to measurement errors rather than to differences in the true fluorescence-lifetime/temperature relations of the two films. The largest error comes from small amounts of excitation illumination reflected by the phosphor and

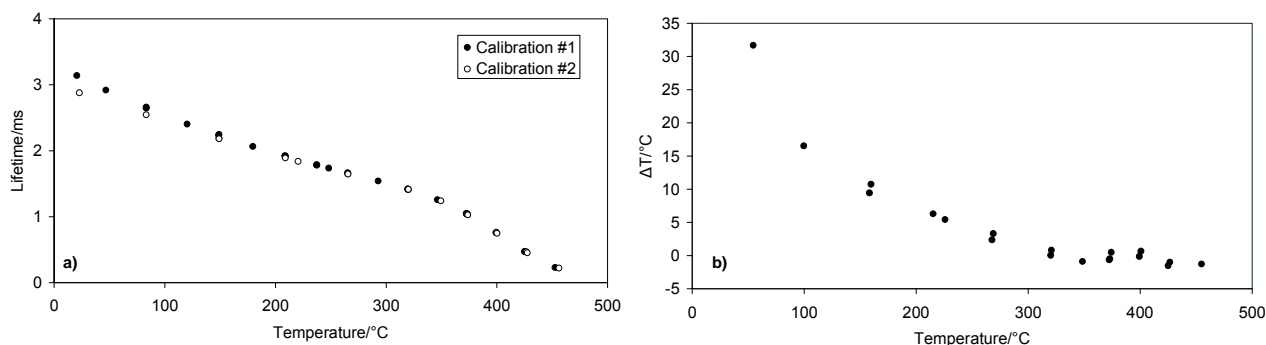


Figure 4. a) Fluorescence-lifetime/temperature relations for two different films of the same phosphor batch. b) Resulting difference in temperatures measured by these two films.

detected by the photomultiplier despite the narrow-band interference filter below it. This background radiation causes systematic errors in the phase-shift measurements. The error is most significant at the lowest temperatures, where the intensity of the fluorescence radiation is lowest. The calibration differences shown in Fig. 4b are most likely due to differences in the thicknesses of the two phosphor films; the resulting fluorescence intensity differences at a given temperature yield different errors in the phase-shift measurements. Figure 4b provides a good estimate of the temperature-measurement uncertainties of present system. However, an improved optical arrangement (e.g. monochromatic excitation illumination) would probably lower this uncertainty.

IV. Temperature Measurements on Microhotplates

The microdevice studies were performed on a chip containing a four-element (each $100\ \mu\text{m} \times 100\ \mu\text{m}$) microhotplate array. The microhotplates were multilayer structures based on a silicon wafer, and included a serpentine-patterned doped-boron polysilicon heater and titanium nitride top electrical contacts. The devices are described in further detail in Ref. 15. To coat the surface of the microhotplates with $\text{Mg}_4(\text{F})\text{GeO}_6:\text{Mn}$, the phosphor was mixed with a low-viscosity (110 centistokes), high-decomposition-temperature ($> 220\ ^\circ\text{C}$) silicone oil. A small drop of this mixture was placed at the end of a $25\ \mu\text{m}$ AlSi wire held by a manual wire bonder machine used to place the drop over the microhotplates. The drop was slowly lowered until it was spread over the surface of the microhotplate through wicking. The heaters of the microhotplates were powered by a DC power supply.

After the phosphor was calibrated and the control tests described in Section III were conducted, the phosphor calibration system was removed from the fluorescence microscope and replaced by the microhotplate chip. Temperature measurements were then made of the surface of one of the microhotplates using fluorescence-lifetime thermometry. The microscope magnification was $100\times$, and the microhotplate filled most of the field of view. Because the entire microhotplate was illuminated, the temperature measured was an average temperature for the surface. Shown in Figure 5 are temperature measurements of one of the microhotplates, where the applied power was held constant over a period of nearly two hours. The measurements show the temperature of the microhotplates to be constant to within $0.2\ ^\circ\text{C}$.

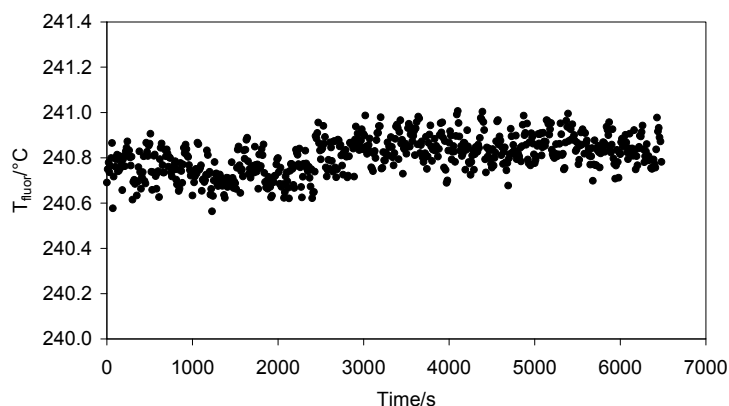


Figure 5. Temperature measurements (using fluorescence-lifetime thermometry) made of the surface of a microhotplate with a constant power applied to it. The temperature is shown to be steady to within 0.2 °C.

Figure 6 illustrates the short-term reproducibility of temperatures achieved when the heat applied to the microhotplates was cycled. The applied voltage was cycled between 0 V and 6 V several times with periods of ~200 s. This resulted in temperatures changing from room temperature to ~240 °C as shown in Fig. 6a. Figure 6b shows the data of Fig. 6a, focusing on the higher temperature region. Repeatability of the temperatures reached by the microhotplates is within 0.2 °C, the resolution of these measurements.

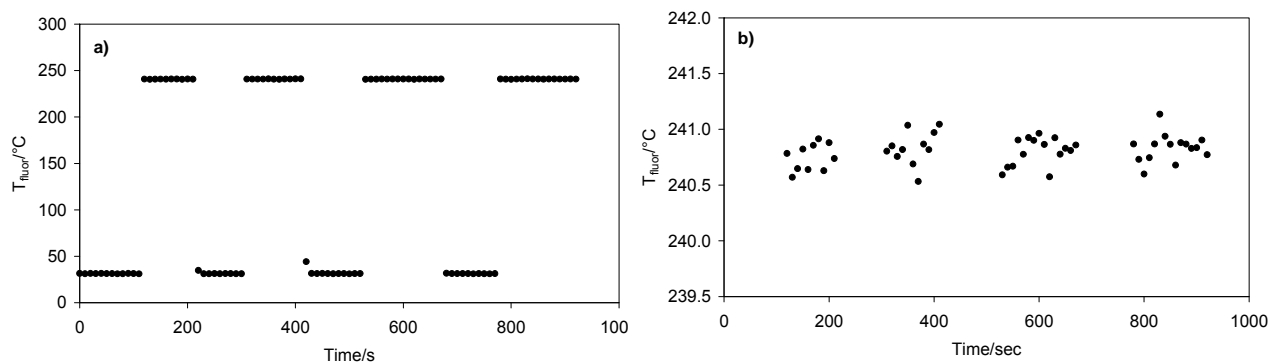


Figure 6. Demonstration of short-term repeatability of temperatures reached by a microhotplate, with temperatures measured by fluorescence lifetime thermometry. In a) the surface temperature of the microhotplate is shown as a function of time. In b) the data of a) is shown with a focus on the temperature region around 240 °C.

Fluorescence thermometry was also used to measure thermal response times for the microhotplates. Fluorescence-lifetime thermometry was not directly used because it cannot measure temperatures in thermal cycles whose period is comparable to or smaller than the lifetime itself. Instead, it was used in conjunction with fluorescence-intensity thermometry, which is not bound by the above constraint.

Fluorescence intensity is also a function of temperature, and the temperature/fluorescence-intensity relations can be used to measure temperature [5]. Fluorescence-lifetime thermometry is considered more accurate and preferable because fluorescence intensity is environment-dependent. However, fluorescence-lifetime thermometry can be used to perform *in situ*

calibrations for fluorescence-intensity thermometry when the temperature is steady. The results of such a calibration on the $\text{Mg}_4(\text{F})\text{GeO}_6:\text{Mn}$ phosphor coating on a microhotplate are shown in Fig. 7. The intensity increases monotonically with temperature over the calibration range. A polynomial fit was made to the results of Fig. 7 to obtain the temperature as a function of intensity.

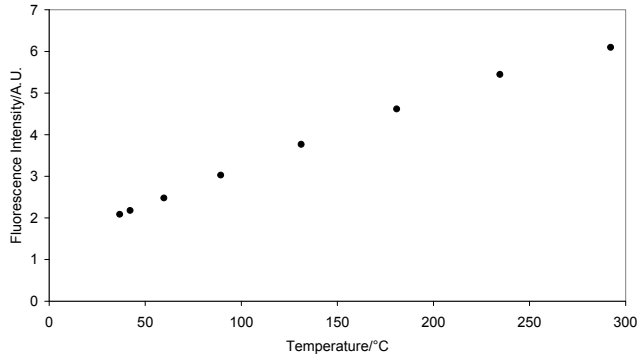


Figure 7. Measurements of the fluorescence intensity (in arbitrary units) as a function of temperature for a $\text{Mg}_4(\text{F})\text{GeO}_6:\text{Mn}$ phosphor coating on a microhotplate under steady heating. The temperature was determined using fluorescence-lifetime thermometry

In order to measure the thermal response of the microhotplate, its temperature was cycled between room temperature and 220 °C with a frequency of 10 Hz by driving it with a square-wave power source. The microhotplate surface temperature was determined as a function of time using the fluorescence intensity, which was measured on a digital oscilloscope. The intensity data was downloaded to a computer and converted to temperatures. A plot of the temperature as a function of time is shown in Figure 8a. Subsequently a nonlinear least-squares fit was made to the decaying portion of the data. The equation used was

$$I(t) = Ae^{-t/t_0} + C, \quad (2)$$

where I is the fluorescence intensity, t is the time, A and C are the amplitude and offset constants, and t_0 is the thermal response time of the microhotplate. The fit determined the thermal response time to be (8.41 ± 0.02) ms.

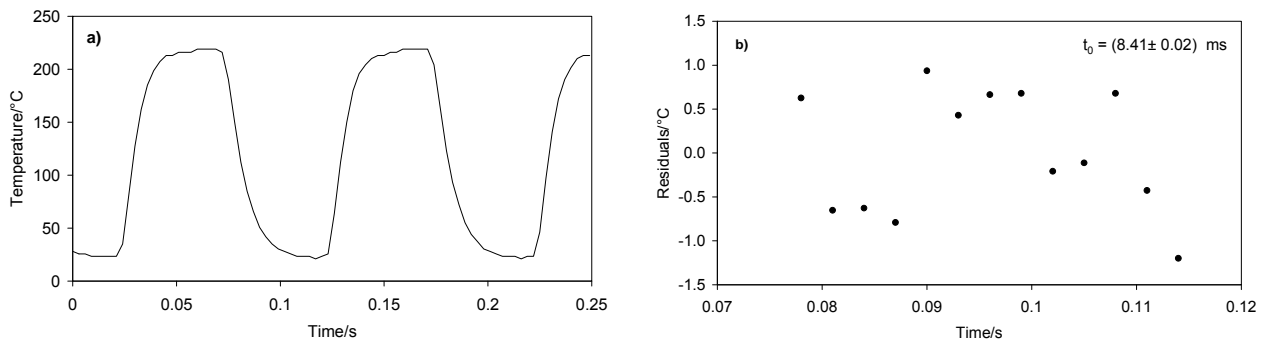


Figure 8. Measurement of the thermal response of a microhotplate driven with a square-wave power input. a) The temperature of the microhotplate measured as a function of time using fluorescence-intensity thermometry. b) Residuals from the nonlinear least-squares fit of Eq. 2 to a portion of the data of a) showing exponential decay. The thermal response was determined to be $t_0 = (8.41 \pm 0.02)$ ms.

This work demonstrates the potential of fluorescence thermometry for characterizing the performance of microhotplate-based conductometric gas sensors and related MEMS devices. This method can be refined to enable higher resolution temperature measurements on the microhotplates, making it possible to measure (and minimize) temperature gradients on them. For example, Herman et al. [8] used a collection of lenses and diaphragms to focus the LED light onto an area of diameter 15 μm in their fluorescence microscope to achieve a resolution of this size. Also, Izaguirre et al. [7] have used the electron beam of a scanning electron microscope to perform fluorescence lifetime thermometry with a spatial resolution of less than 10 μm . Fluorescence lifetime imaging microscopes [9] and fluorescence intensity imaging microscopes [10] have been developed and can be used for thermal imaging. Such measurements will be helpful in characterizing the operation and optimizing the design of microhotplates as chemical sensors.

Acknowledgements: We thank Steve Allison for helpful discussions and guidance. We also thank Jim Maslar, Robert F. Berg, Joseph T. Hodges, Howard Yoon and John Lawall for their equipment loans that made this project possible.

References

- 1 S. Semancik and R. Cavicchi, Kinetically controlled chemical sensing using micromachined structures, *Acc. of Chem. Res.* 31 (1998) 279-287.
- 2 R.E. Cavicchi *et al.*, Fast temperature programmed sensing for micro-hotplate gas sensors, *IEEE Elec. Dev. Lett.* 16 (1995) 286-288.
- 3 C.J. Taylor and S. Semancik, Use of microhotplate arrays as microdeposition substrates for materials exploration, *Chem. Mater.* 14 (2002) 1671-1676.
- 4 S. Semancik, in Xiang and Takeuchi (ed.), *Combinatorial Materials Synthesis*, Marcel Dekker, Inc., New York, 2003, Ch. 9, pp. 263-295.
- 5 S.W. Allison and G.T. Gillies, Remote thermometry with thermographic phosphors, *Rev. Sci. Instrum.* 68 (1997) 2615-2650.
- 6 P. Kolodner and J. A. Tyson, Microscopic fluorescent imaging of surface temperature profiles with 0.01 °C resolution, *Appl. Phys. Lett.* 40 (1982) 782-784; P. Kolodner and J. A. Tyson, Remote thermal imaging with 0.7- μ m spatial resolution using temperature-dependent fluorescent thin films, *Appl. Phys. Lett.* 42 (1983) 117-119.
- 7 F. Izaguirre, G. Csanky, and G.F. Hawkins, Temperature measurements with micrometer spatial resolution, *Rev. Sci. Instrum.* 62 (1991) 1916-1920.
- 8 P. Herman *et al.*, Frequency-domain fluorescence microscopy with the LED as a light source, *J. Microsc.* 203 (2001) 176-181.
- 9 T.W.J. Gadella Jr., T.M. Jovin, and R.M. Clegg, Fluorescence lifetime imaging microscopy (FLIM): spatial resolution of microstructures on the nanosecond time scale, *Biophysical Chemistry* 48 (1993) 221-238.
- 10 N. Boyer *et al.*, Temperature distribution over a GaAs heterojunction bipolar transistor measured by fluorescent microthermal imaging, *J. Vac. Sci. Technol. A* 18 (2000) 754-756.
- 11 S.W. Allison, M.R. Cates, Excitation of thermographic phosphors using a blue light emitting diode: spectral characteristics and instrumentation applications, *Rev. Sci. Instrum.* 73 (2002) 1832-1834.
- 12 J.R. Lakowitz, *Principles of Fluorescence Spectroscopy*, Kluwer Academic/Plenum Publishers, New York, 1999, pp. 142-144.
- 13 Certain commercial companies are identified in this paper in order to adequately identify the equipment used. Such identification does not imply recommendation or endorsement by the National Institute of Standards and Technology, nor does it imply that the identified commercial sources are necessarily the best available for the purpose
- 14 ASTM, *2004 Annual Book of ASTM Standards* Vol. 14.03, ASTM, Philadelphia, 2004, pp. 117-308.
- 15 S. Semancik *et al.*, Microhotplate platforms for chemical sensor research, *Sens. Actuators B* 77 (2001) 579-591.